Micellization Temperature and Pressure for Polystyrene-*block*-polyisoprene in Subcritical and Supercritical Propane

W. Winoto, H. Adidharma, Y. Shen, and M. Radosz*

Soft Materials Laboratory, Department of Chemical and Petroleum Engineering, University of Wyoming, Laramie, Wyoming 82071-3295

Received May 5, 2006; Revised Manuscript Received August 1, 2006

ABSTRACT: Polystyrene-*block*-polyisoprene forms micelles in supercritical and subcritical propane upon cooling and decompression. These micelles decompose upon heating and compression. At constant polymer concentration, the micellization points, both isobaric and isothermal, fall around a decreasing boundary curve in pressure−temperature coordinates. This micellization boundary curve lies above the copolymer cloud-point curve and below the free-polystyrene cloud-point curve. At the onset of micellization, a trace of free polystyrene can cause a characteristic scattering peak as it precipitates upon cooling or decompression or both.

Introduction

Polymers of complex but well-defined backbone architecture, such as block copolymers, play an increasingly important role in nanostructure materials technology. Most practical applications exploit their capacity to self-assemble and to form nanophase-separated systems.[1,2] The graft and block copolymers have been applied, for example, in the areas of nanotechnology,[1,3] amphiphilic surfactants,[4] thermoplastic elastomers,[2] dendrimers,[5,6] membrane technology,[7] and drug delivery,[8,9] just to mention a few recent applications.

Block copolymers of precisely controlled architecture and uniform properties, such as molecular weight, chain structure, repeating unit structure, and functionality, can be obtained, for example, from anionic living polymerization[10,11] and atom transfer radical polymerization (ATRP).[12]

Normally, block copolymers are studied in melts and liquid solutions, for example, in dilute liquid solutions using dynamic light scattering to determine the micellization temperature (the temperature at which micelles begin to form or decompose), micelle size, and other properties. For the record, the micellization temperature is often referred to as the critical micelle temperature, but we prefer to avoid this term to avoid confusion with the usual critical phenomena, for example in pure solvents and solutions; we see the micellar to nonmicellar transition (and vice versa) as a point on a micellar (nanophase) boundary curve separating the micellar solution from a molecular solution, rather than a true critical point.

Among numerous references on the subject of block copolymer micellization, a relevant example is that published by Lodge et al.[13] on polystyrene-*block*-polyisoprene micellization in liquid solvents. They attributed a distinct scattering intensity peak observed at the onset of micellization upon cooling to the precipitation of a free-polystyrene trace just before its absorption by the micelle core.

This work is motivated by the need to understand how such block copolymer micellization will respond to pressure in near critical fluid solutions, where, instead of an essentially incompressible liquid solvent, one uses a compressed and highly compressible fluid near its critical temperature, either above or below its critical temperature. Such near critical solvents are easier to recover, less viscous, pressure sensitive, and hence allow for unique processing, purification and fractionation approaches, not to mention creative ways to control micellization.[14] An example of a near critical solvent that has been applied to oligomers, polymers, and random copolymers is propane.[15−22] However, no near critical hydrocarbon solvent has been applied to block copolymers yet. One of the few examples of diblock copolymer micellization in supercritical carbon dioxide is provided by the work of DeSimone's group[23−25] and Chu's group,[26] who reported micellization densities, some of which were also later calculated by Colina et al.[27] No such data are available for block copolymers in near critical hydrocarbons, such as small alkanes.

The goal of this work is to explore and characterize the micellization of polystyrene-*block*-polyisoprene (PS-*b*-PIP) in near critical propane, including the micellization temperature determined upon cooling at constant pressure (the "critical micelle temperature") and the micellization pressure determined upon decompression at constant temperature (the "critical micelle pressure"). Like other alkanes, near critical propane is a relatively poor solvent for polystyrene[22] and a relatively good solvent for polydienes,[28] and therefore the PS-*b*-PIP micelles are expected to have a polystyrene core and polyisoprene corona.

Experimental Section

Materials. The PS(11.5K)-*b*-PIP(10.5K) sample was synthesized by Polymer Source, Inc., via living anionic polymerization with sequence addition of styrene followed by isoprene. The number-average molecular weight is 11 500 and 10 500 g/mol for the styrene and isoprene blocks, respectively. The polydispersity index of the diblock is 1.04. The isoprene block is about 90% of the 1,4-addition type. The PS(9K) and PIP(10K) homopolymer samples were also synthesized via living anionic polymerization. The PS(9K) was synthesized in our lab, and the PIP(10K) (95% 1,4-addition) was synthesized by Polymer Source, Inc. The number-average molecular weight and the polydispersity index are 8 830 g/mol and 1.13 for PS(9K) and 10 100 g/mol and 1.04 for PIP(10K). The propane is 99.0% grade from Matheson Gas Product, Inc.

Cloud-Point and Micellization Experiments. The cloud point refers to an initial stage of the bulk phase separation in a molecular or macromolecular solution, induced either by changing temperature at constant pressure, which results in the cloud-point temperature,

* Corresponding author. E-mail: radosz@uwyo.edu.

10.1021/ma061012t CCC: $33.50
Published on Web 10/18/2006

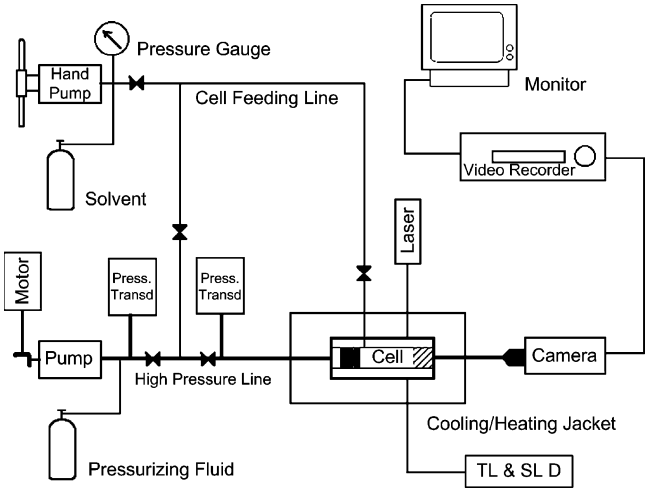

Figure 1. A simplified schematic of the apparatus.

or by changing pressure at constant temperature, which results in the cloud-point pressure. The micellization temperature (MT) refers to the highest temperature at which micelles can be formed upon cooling at constant pressure. (We shall explain further that there are other systems in which micelles can be formed upon heating, where MT will be the lowest temperature at which micelles can be formed.) The micellization pressure (MP) refers to the highest pressure at which micelles can be formed upon decompression at constant temperature. The nanosized micelle-containing phase is referred to as the micellar solution, in contrast to the molecular solution observed following micelle decomposition.

The cloud-point, MT, and MP transitions are measured in a small (about 1 cm^3 in volume) high-pressure variable-volume cell coupled with transmitted- and scattered-light intensity probes and with a borescope for visual observation of the phase transitions. A simplified schematic of the apparatus is shown in Figure 1. This apparatus is equipped with a data acquisition and control systems described elsewhere.[21] The control system allows not only for constant temperature and pressure measurements but also for decreasing and increasing temperature and pressure measurements at a constant rate. The cloud points reported in this work are detected with a transmitted-light intensity probe. The micellization points are detected with a scattered-light intensity probe. A detailed description of the apparatus and of its transmitted-light intensity probe is given elsewhere.[17,21]

The cell has a floating piston, which can change the volume of the cell, to compress or decompress the mixture to a desired pressure, without having to change the mixture composition. A known amount of the copolymer (0.5 wt %) and propane is loaded into the cell, which is then brought to and maintained at a desired pressure and temperature at which copolymer can be dissolved. After the mixture is well equilibrated in a one-phase region for at least 90 min by stirring at constant temperature and pressure, there are two choices: an isothermal experiment and an isobaric experiment. In the isothermal experiment, the pressure is decreased slowly, while in the isobaric experiment the temperature is decreased slowly, until the solution turns turbid, which indicates the onset of phase separation. In this study, a pressure rate as low as 15 bar/min is chosen to obtain a reproducible cloud point as suggested by a previous study.[29] The cloud points are reproducible to within ±3 bar most of the time, except at the highest pressure for PS(9K), where the error can be as high as ±30 bar.

Upon crossing the bulk phase boundary from the one-phase side, the transmitted-light intensity (TLI) starts decreasing. Conversely, upon approaching the phase boundary from the two-phase side, TLI starts increasing. A new data point is taken after reequilibrating the mixture for 15 min in the one-phase region, well above the expected cloud point temperature and pressure. In all cases, the TLI data are stored and analyzed as a function of time, temperature, and pressure. The cloud point pressure in this work is taken as the inflection point on the TLI curve, which corresponds to a peak on its first derivative.

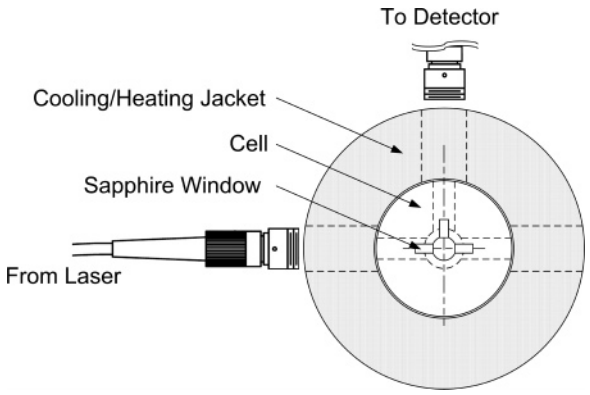

Figure 2. Optical fiber interface.

Table 1. Nominal and Measured Diameters of Particle Standards

nominal diameter (nm)		measured diameter range (av) (nm)	particle concn (wt %)
20	21 ± 1.5	19.3−22.8 (20.6)	0.50
70	73 ± 2.6	56.5−73.6 (66.0)	0.12
200	200 ± 30	173.4−240.4 (201)	0.012

The micelle formation is probed using high-pressure dynamic light scattering. The scattered-light intensity and the hydrodynamic radius sharply increase upon crossing a micellization boundary at constant pressure (MT) or at constant temperature (MP). In this work, we focus on a low concentration range where it is safe to assume spherical micelles.

For these measurements, we couple our high-pressure equilibrium cell described in the previous section with an argon ion laser (National Laser) model 800BL operating at λ of 488 nm and a Brookhaven BI-9000AT correlator. The coherence area is controlled with a pinhole placed before the detector. The laser and detector are interfaced with the high-pressure cell via optical fibers produced by Thorlabs, as shown in Figure 2. The high-pressure optical fiber interface design is different from but inspired by the approach described by Koga et al.[30] The scattered-light intensity is measured and recorded for both isothermal experiments (upon decreasing or increasing pressure at a rate of 30−60 bar/min) and isobaric experiments (upon decreasing or increasing temperature at a rate of 0.4−2.0 °C/min).

Results and Discussion

Dynamic Light Scattering Tests. Three polystyrene particle standards are used to test the light scattering probe: (1) with nominal diameter of 20 nm from Duke Scientific Corp., (2) with nominal diameter of 70 nm from Duke Scientific Corp., and (3) with nominal diameter of 200 nm from Sigma Aldrich. Each particle standard is dispersed in distilled water and loaded into the cell. The temperature is kept constant at 25 °C using a water bath circulator for 15 min before scattered-light intensity is measured. About 5 min measurements are taken at ambient pressure for each size standard at least five times. The results are found to fall within a ±10% band around the nominal diameter, as shown in Table 1.

The hydrodynamic radius, R_H, the radius of an equivalent sphere that gives the same frictional resistance to linear translation as the copolymer aggregate, is estimated from the Stokes−Einstein equation:[31]

$$R_H = \frac{kT}{6\pi\eta_0 D} \quad (1)$$

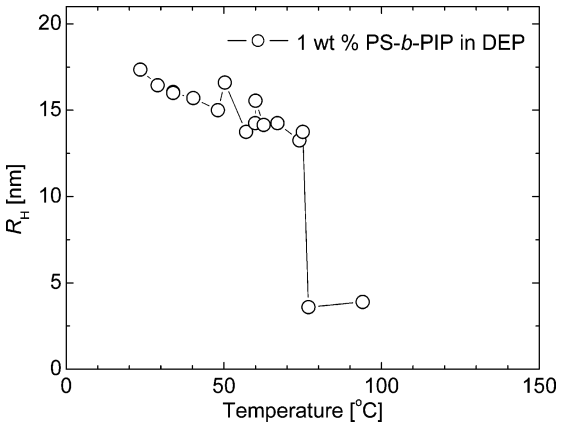

Figure 3. Hydrodynamic radius of 1 wt % PS(11.5K)-*b*-PIP(10.5K) solution in DEP as a function of temperature.

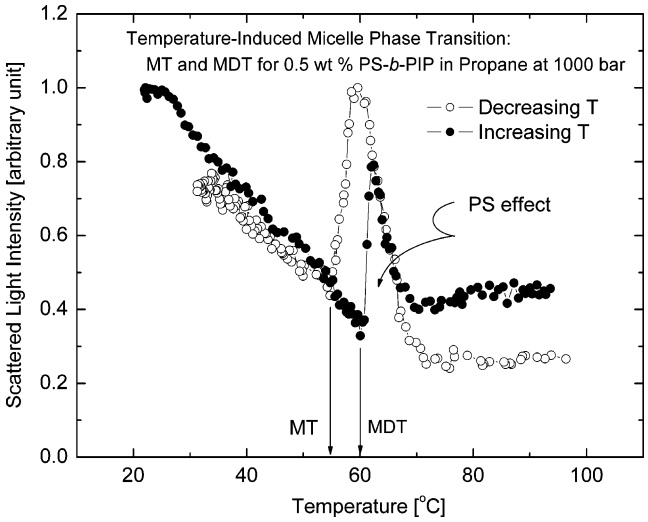

Figure 4. Scattered-light intensity of 0.5 wt % PS(11.5K)-*b*-PIP(10.5K) solution in propane as a function of temperature; MT is the micellization temperature, and MDT is the micelle decomposition temperature.

where k is the Boltzmann constant, η_0 is the solvent viscosity, T is the absolute temperature, and D is the diffusion coefficient determined from dynamic light scattering.

Initially, we measure the hydrodynamic radius of 1 wt % PS(11.5K)-*b*-PIP(10.5K) solution in diethyl phthalate (DEP) at ambient pressure. The viscosity, density, and refractive index of diethyl phthalate are taken from Lorenzi et al.[32] Figure 3 shows the measured hydrodynamic radius as a function of temperature, from which the MT is found to be about 77 °C, which is consistent with the results reported by Lodge et al. for PS(8K)-*b*-PIP(7K) at 60 °C[13] and for PS(15K)-*b*-PIP(13K) at 90 °C.[33] Having reproduced the published data for PS-*b*-PIP in an incompressible solvent at ambient pressure, we characterize the same diblock type but in a strongly compressible solvent, such as near critical propane, at high pressures, using the scattered-light intensity rather than R_H as a micellization probe. Hence, we do not need the viscosity, density, and refractive index for propane.

Micellization Temperature. Toward this end, we first plot the scattered-light intensity vs temperature to determine MT. Initially, we dissolve 0.5 wt% PS(11.5K)-*b*-PIP(10.5K) in propane above its cloud point, say at about 1000 bar and 100 °C. Then, while decreasing the temperature, we find MT to be 54.8 °C, as shown in Figure 4 with open points. Reassuringly,

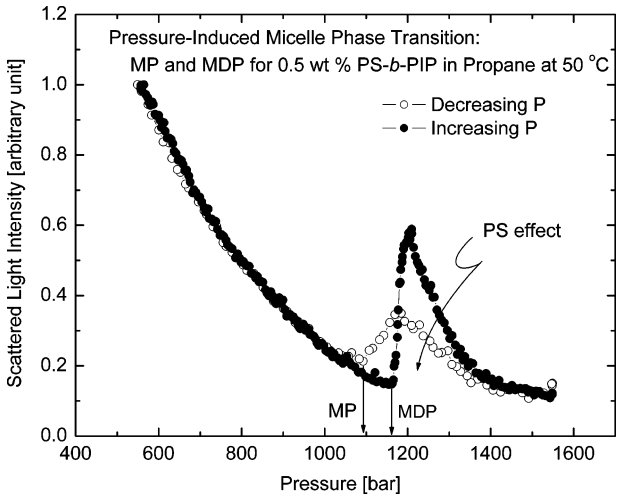

Figure 5. Scattered-light intensity of 0.5 wt % PS(11.5K)-*b*-PIP(10.5K) solution in propane as a function of pressure; MP is the micellization pressure, and MDP is the micelle decomposition pressure.

we find a scattered-intensity peak referred to as "anomalous micellization" in the literature. Lodge et al.[13] reported data supporting a hypothesis that this peak reflects a trace of free PS that precipitates from solution before being absorbed by the micelle core. As proven by Lodge et al.,[13] this peak can be eliminated by repeated fractionation, but, since it does not alter MT, we simply use it to estimate MT, as shown in Figure 4. The curve with filled points in Figure 4 represents a micelle decomposition experiment upon heating the micellar solution. The heating-induced micelle decomposition temperature (MDT) is about 5 °C higher than the cooling-induced MT, which is reproducible at these conditions. At lower pressures (lower densities), however, this temperature difference tends to be lower.

Micellization Pressure. Next, we explore isothermal micellization upon decompression that leads to micellization pressure (MP) and isothermal micelle decomposition upon compression that leads to micelle decomposition pressure (MDP), by plotting the scattered-light intensity vs pressure. A sample result for the same system, that is 0.5 wt % PS(11.5K)-*b*-PIP(10.5K) in propane, is shown in Figure 5 with open points for decompression and with filled points for compression. Interestingly, MP is preceded by an analogous peak attributable to a small fraction of free PS that, having reached its cloud-point pressure, momentarily precipitates before being absorbed by the micelle core. As for MT, we use this peak to estimate MP. Also, similar to MT, there is a reproducible difference between MP and MDP; about 6% (70 bar or so) for the example in Figure 5, which tends to decrease with increasing temperatures (decreasing densities).

For this system, the micelles decompose upon increasing pressure beyond MP because, while increasing pressure increases the solvent capacity for both blocks, it decreases the solvent capacity *difference* between the two blocks.

Micellization Pressure−Temperature Boundary. Still for the same system of 0.5 wt % PS(11.5K)-*b*-PIP(10.5K) in propane, all the cloud and micellization boundary points measured in this work are plotted in pressure−temperature coordinates in Figure 6. The curve with star points (top) indicates the cloud points for polystyrene (PS(9K)) alone. A similar curve with diamond points (bottom) indicates the cloud points for polyisoprene (PIP(10K)) alone. Each of these cloud-point curves separates the one-phase (homogeneous solution) region at high pressures from a two-phase region at lower pressures. Their

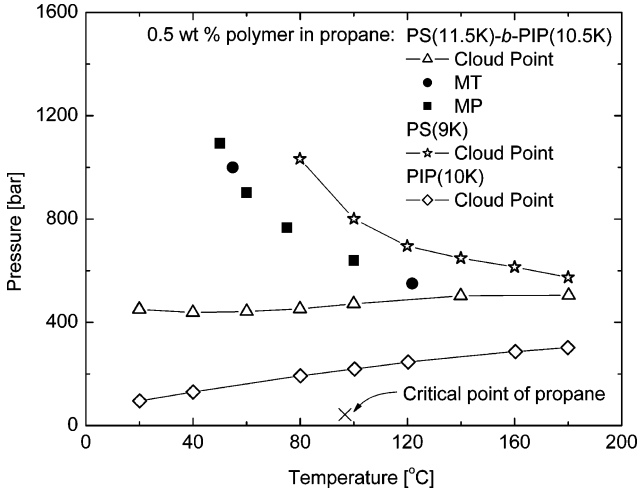

Figure 6. Pressure−temperature phase diagram showing the cloud-point (fluid−liquid) transitions, micellization temperatures (MT, upon isobaric cooling), and micellization pressures (MP, upon isothermal decompression).

slopes suggest that PS(9K) exhibits an upper critical solution temperature (UCST) behavior while PIP(10K) exhibits a lower critical solution temperature (LCST) behavior. The curve with triangles, on the other hand, indicates cloud points for PS(11.5K)-*b*-PIP(10.5K) (again, one phase above, two phases below). Let us note that the cloud point curve for this symmetrical diblock copolymer is closer to the PIP curve at low temperatures and closer to the PS curve at high temperatures.

Figure 6 also shows micellization points, filled circles for MT and filled squares for MP, which cluster around a single micellization boundary curve that resembles the free-PS cloud-point curve. The micellization boundary curve separating the molecular solution region (above) from the micellar solution region (below) should intersect the diblock cloud-point curve below 140 °C because no MP is observed at or above 140 °C.

The micellization boundary curve in Figure 6 suggests that micellization is related to the solution density, but in general, the density *alone* cannot uniquely explain the micellization. For example, in our case, increasing density upon cooling induces micelle formation, but increasing density upon compression induces micelle decomposition. This behavior should be characteristic of core-forming blocks that in their homopolymer state exhibit UCST-like behavior in a given solvent, such as free PS in propane. However, for core-forming blocks that in their homopolymer state exhibit LCST-like behavior in a given solvent, increasing density should *always*, upon cooling *and* compression, induce micelle decomposition. For example, for poly(1,1-dihydroperfluorooctyl acrylate)-*block*-poly(vinyl acetate) in carbon dioxide studied by Zhou et al.,[26] where the core-forming block is poly(vinyl acetate) which exhibits LCST-like behavior in carbon dioxide,[34,35] increasing density *always* favors micelle decomposition, upon cooling and compression.

Finally, the pressure−temperature phase diagram shown in Figure 6 is qualitatively consistent with Lodge et al.'s[13] hypothesis that the PS "anomalous micellization" peak is due to the precipitation of a trace homopolymer that is of the same kind as the core-forming block. Such a precipitation takes place upon crossing the cloud point curve for the PS impurity, which, in turn, must lie below the PS cloud-point curve shown in Figure 6 as the impurity concentration is much lower than that used in our cloud-point experiments.

Conclusion

Polystyrene-*block*-polyisoprene is found to form micelles in supercritical and subcritical propane upon cooling and decompression, which decompose upon heating and compression. At constant polymer concentration, the micellization points, both isobaric and isothermal, fall around a decreasing boundary curve in pressure−temperature coordinates. This micellization boundary curve lies above the copolymer cloud-point curve and below the free-polystyrene cloud-point curve. At the onset of micellization, a trace of free polystyrene is found to cause a characteristic scattering peak as it precipitates upon cooling or decompression or both. A similar scattering peak is observed toward the end of micelle decomposition upon heating and compression, but it is usually slightly shifted relative to the corresponding micellization peak.

Acknowledgment. Jin Sun prepared the polystyrene sample. Michal Banaszak and Mikhail Anisimov provided helpful comments. This work is funded by NSF Grant CTS-0244388.

References and Notes

(1) Hamley, I. W. *The Physics of Block Copolymers*; Oxford University Press: New York, 1998.
(2) Legge, N. R.; Holden, G.; Schroeder, H. E. *Thermoplastic Elastomers*; Hanser Publishers: Munich, 1987.
(3) Böker, A.; Müller, A. H. E.; Krausch, G. *Macromolecules* **2001**, *34*, 7477−7488.
(4) Ydens, I.; Rutot, D.; Degée, P.; Six, J.-L.; Dellacherie, E.; Dubois, P. *Macromolecules* **2000**, *33*, 6713−6721.
(5) Astruc, D.; Chardac, F. *Chem. Rev.* **2001**, *101*, 2991−3023.
(6) Zeng, F.; Zimmerman, S. C. *Chem. Rev.* **1997**, *97*, 1681−1712.
(7) Park, E.-S.; Yoon, J.-S. *J. Appl. Polym. Sci.* **2001**, *82*, 1658−1667.
(8) Uhrich, K. E.; Cannizzaro, S. M.; Langer, R. S.; Shakesheff, K. M. *Chem. Rev.* **1999**, *99*, 3181−3198.
(9) Xu, P.; Tang, H.; Li, S.; Ren, J.; Kirk, E. V.; Murdoch, W. J.; Radosz, M.; Shen, Y. *Biomacromolecules* **2004**, *5*, 1736−1744.
(10) Hadjichristidis, N.; Pitsikalis, M.; Pispas, S.; Iatrou, H. *Chem. Rev.* **2001**, *101*, 3747−3792.
(11) Uhrig, D.; Mays, J. W. *J. Polym. Sci., Part A: Polym. Chem.* **2005**, *43*, 6179−6222.
(12) Matyjaszewski, K.; Xia, J. *Chem. Rev.* **2001**, *101*, 2921−2990.
(13) Lodge, T. P.; Bang, J.; Hanley, K. J.; Krocak, J.; Dahlquist, S.; Sujan, B.; Ott, J. *Langmuir* **2003**, *19*, 2103−2109.
(14) Kendall, J. L.; Canelas, D. A.; Young, J. L.; DeSimone, J. M. *Chem. Rev.* **1999**, *99*, 543−563.
(15) Chan, A. K. C.; Hemmingsen, P. V.; Radosz, M. *J. Chem. Eng. Data* **2000**, *45*, 362−368.
(16) Chan, A. K. C.; Radosz, M. *Macromolecules* **2000**, *33*, 6800−6807.
(17) Chan, A. K. C.; Russo, P. S.; Radosz, M. *Fluid Phase Equilib.* **2000**, *173*, 149−158.
(18) Chan, K. C.; Adidharma, H.; Radosz, M. *Ind. Eng. Chem. Res.* **2000**, *39*, 3069−3075.
(19) Condo, P. D., Jr.; Colman, E. J.; Ehrlich, P. *Macromolecules* **1992**, *25*, 750−753.
(20) Kermis, T. W.; Li, D.; Guney-Altay, O.; Park, I.-H.; Zanten, J. H. v.; McHugh, M. A. *Macromolecules* **2004**, *37*, 9123−9131.
(21) Łuszczyk, M.; Radosz, M. *J. Chem. Eng. Data* **2003**, *48*, 226−230.
(22) Tan, S. P.; Meng, D.; Plancher, H.; Adidharma, H.; Radosz, M. *Fluid Phase Equilib.* **2004**, *226*, 189−194.
(23) Buhler, E.; Dobrynin, A. V.; DeSimone, J. M.; Rubinstein, M. *Macromolecules* **1998**, *31*, 7347−7355.
(24) Triolo, A.; Triolo, F.; Celso, F. L.; Betts, D. E.; McClain, J. B.; DeSimone, J. M.; Wignall, G. D.; Triolo, R. *Phys. Rev. E* **2000**, *62*, 5839−5842.
(25) Triolo, R.; Triolo, A.; Triolo, F.; Steytler, D. C.; Lewis, C. A.; Heenan, R. K.; Wignall, G. D.; DeSimone, J. M. *Phys. Rev. E* **2000**, *61*, 4640−4643.
(26) Zhou, S.; Chu, B. *Macromolecules* **1998**, *31*, 7746−7755.
(27) Colina, C. M.; Hall, C. K.; Gubbins, K. E. *Fluid Phase Equilib.* **2002**, *194−197*, 553−565.
(28) Winoto, W.; Adidharma, H.; Sun, J.; Shen, Y.; Radosz, M. Phase Behavior of Polybutadiene-*block*-polystyrene in Near-Critical and Supercritical Propane. In *International Symposium on Supercritical Fluids*, Orlando, FL, 2005.
(29) Plancher, H.; Adidharma, H.; Radosz, M. High-Pressure Fluid-Liquid and Solid-Liquid Equilibria of Polyethylene, Polystyrene, and Polyethylene-*co*-polystyrene in Propane. In *American Institute of Chemical Engineers Annual Meeting*, Indianapolis, IN, 2002.

(30) Koga, T.; Zhou, S.; Chu, B.; Fulton, J. L.; Yang, S.; Ober, C. K.; Erman, B. *Rev. Sci. Instrum.* **2001**, *72*, 2679−2685.
(31) Mazer, N. A. Laser Light Scattering in Micellar Systems. In *Dynamic Light Scattering*; Pecora, R., Ed.; Plenum Press: New York, 1985.
(32) Lorenzi, L. D.; Fermeglia, M.; Torriano, G. *J. Chem. Eng. Data* **1997**, *42*, 919−923.
(33) Lodge, T. P.; Pudil, B.; Hanley, K. J. *Macromolecules* **2002**, *35*, 4707−4717.
(34) Rindfleisch, F.; DiNoia, T. P.; McHugh, M. A. *J. Phys. Chem.* **1996**, *100*, 15581−15587.
(35) Shen, Z.; McHugh, M. A.; Xu, J.; Belardi, J.; Kilic, S.; Mesiano, A.; Bane, S.; Karnikas, C.; Beckman, E.; Enick, R. *Polymer* **2003**, *44*, 1491−1498.

MA061012T